한국지진공학회 논문집 | 제10권 제6호 (통권 제52호) | 2006년 12월, pp. 79~91

Baseline-Free Crack Detection in Steel Structures using Lamb Waves and PZT Polarity

램파와 압전소자 극성을 사용한 강구조의 실시간 균열손상 감지기법 개발

김승범[1] · 손 훈[2]

Kim, Seung-Bum · Sohn, Hoon

국문 요약 >> 이 연구에서는 강교량과 같은 토목 구조물에서 유도파의(Guided waves) 한 종류인 램파(Lamb wave)를 이용하여 실시간으로 균열손상을 감지할 수 있는 새로운 비파괴 검사방법을 제안한다. 기존의 유도파를 이용한 기술들은, 손상을 감지하기 위해 비손상 상태의 자료를 저장하고 이를 새로이 얻어진 결과와 비교하는 방법을 사용함으로써 잠재적인 손상을 진단해 왔다. 그러나, 공용중인 강구조물은 다양한 하중 뿐 아니라 상시로 변화하는 자연환경에 노출되어 있기 때문에 동일한 비손상 상태의 응답을 얻는 것이 매우 어려우며 이러한 방법을 적용할 경우 오보(false alarm)의 우려도 매우 높다고 할 수 있다. 따라서 이 연구에서는 보다 안정적인 손상감지기법을 개발하기 위해 기존에 얻어진 초기치를 이용하지 않으면서 실시간으로 손상 여부를 판단할 수 있는 방법을 제안하고자 한다. 이 연구에서 제안된 감지 기술은, 압전소자의 극성과 판파의 특성을 이용하는 것으로 얇은 판의 양면에 부착된 압전소자를 통하여 균열손상에 의한 신호를 선택적으로 감지해 내는 데에 그 목적이 있다. 균열이 발생한 판에서 진행하는 판파는 균열로 인한 판의 두께변화로 인해 모드 변화를 일으키게 되는데, 제안된 감지기법으로 이러한 모드 변화만을 선택적으로 추출할 수 있다. 다양한 수치해석과 실험을 통해 이 연구에서 제안된 손상감지기법의 효율성과 적용성을 입증한다.

주요어 램파, 균열손상 감지, 비파괴 검사, 모드 변이, 압전소자 극성

ABSTRACT >> A new methodology of guided wave based nondestructive testing (NDT) is developed to detect crack damage in civil infrastructures such as steel bridges without using prior baseline data. In conventional guided wave based techniques, damage is often identified by comparing the "current" data obtained from a potentially damaged condition of a structure with the "past" baseline data collected at the pristine condition of the structure. However, it has been reported that this type of pattern comparison with the baseline data can lead to increased false alarms due to its susceptibility to varying operational and environmental conditions of the structure. To develop a more robust damage diagnosis technique, a new concept of NDT is conceived so that cracks can be detected without direct comparison with previously obtained baseline data. The proposed NDT technique utilizes the polarization characteristics of the piezoelectric wafers attached on the both sides of the thin metal structure. Crack formation creates Lamb wave mode conversion due to a sudden change in the thickness of the structure. Then, the proposed technique instantly detects the appearance of the crack by extracting this mode conversion from the measured Lamb waves even at the presence of changing operational and environmental conditions. Numerical and experimental results are presented to demonstrate the applicability of the proposed technique to crack detection.

Key words lamb wave, crack detection, nondestructive testing, mode conversion, piezoelectric polarization

1. Introduction

There has been an increasing demand in using Structural Health Monitoring (SHM) and Nondestructive Testing (NDT) techniques for continuous monitoring of civil infrastructures to prevent sudden failure from catastropic disasters such as earthquakes. For SHM/NDT, guided waves have received a great deal of attention and have been a topic of considerable interest, because they can propagate over considerable distances with little attenuation. Conventional guided wave studies have focused on schemes where baseline signals are measured so that changes from the baseline can be detected. However, there are significant technical challenges to realizing this pattern comparison.

[1] Graduate Student, Department of Civil & Environmental Engineering, Carnegie Mellon University, Pittsburgh, PA, 15213

[2] Assistant Professor, Department of Civil & Environmental Engineering, Carnegie Mellon University, Pittsburgh, PA, 15213
(대표저자: hsohn@cmu.edu)

본 논문에 대한 토의를 2007년 2월 28일까지 학회로 보내 주시면 그 결과를 게재하겠습니다.

(논문접수일 : 2006. 10. 10 / 심사종료일 : 2006. 11. 23)

For instance, structural defects typically take place long after the initial baseline are collected, and other operational and environmental variations of the system can produce significant changes in the measured response, masking any potential signal changes due to structural defects.

As an alternative that can overcome the drawbacks of the conventional NDT methods, a new concept of NDT technique, which does not rely on previously obtained baseline data, is proposed for crack detection. In a thin elastic medium such as a metal plate, the formation of a crack causes the conversion of the propagation waves to other modes. In this paper, a technique that can isolate this mode conversion is developed using the poling directions of piezoelectric materials such as Lead Zirconate Titanate (PZT). The uniqueness of the proposed crack damage detection technique is that this mode conversion due to a crack is instantly identified without using prior baseline data. By removing the dependency on the prior baseline data, the proposed damage detection system becomes less vulnerable to operational and environmental variations that might occur throughtout the life span of the structures being monitored.

This paper is organized as follows. First, the polarization process of crystalline materials is briefly described. Then, the effect of a PZT polarization direction on Lamb wave measurement is investigated, and the proposed reference-free diagnosis technique is developed based on the PZT poling directions. Furthermore, a thresholding technique is developed to make the proposed NDT technique less sensitive to variations in PZT size, bonding condition and alignment. Finally, experimental tests as well as numerical simulations are executed to investigate the applicability of the proposed NDT technique to crack detection.

2. Theoretical Development

2.1 Piezoelectric Material and its Polarization Characteristics

Piezoelectric materials are natural or artificially polarized ceramics which have piezoelectricity.[1] These materials develop an electrical charge or voltage when a mechanical pressure is applied, which is the simplest description of piezoelectricity. Conversely, piezoelectric materials produce deformation (strain) when exposed to an applied electric field. Due to this unique nature of the piezoelectric materials, they are commonly used as both sensors and actuators in many applications.[2] For instance, wafer-type piezoelectric materials such as PZT are commonly used for exciting and measuring guided waves for SHM and NDT applications (Giurgiutiu and Zagrai[3]). In some natural ceramic materials such as quartz, crystal cells that behave similarly to electric dipoles are oriented along the crystal axes. However, other crystalline materials often have random orientation of the dipoles at the initial state, and they are polarized during a thermal poling process.[1] In the first stage, a crystalline material with randomly oriented dipoles is slightly warmed up below its Curie temperature [Figure 1 (a)]. After a strong electric field E is applied to the crystalline material, the dipoles in the material align along the field lines [Figure 1 (b)]. Finally, the material is cooled down, and the electric field is removed [Figure 1 (c)]. The polarization of the material is permanently maintained as long as the poled material stays below its Curie temperature. The overall behavior

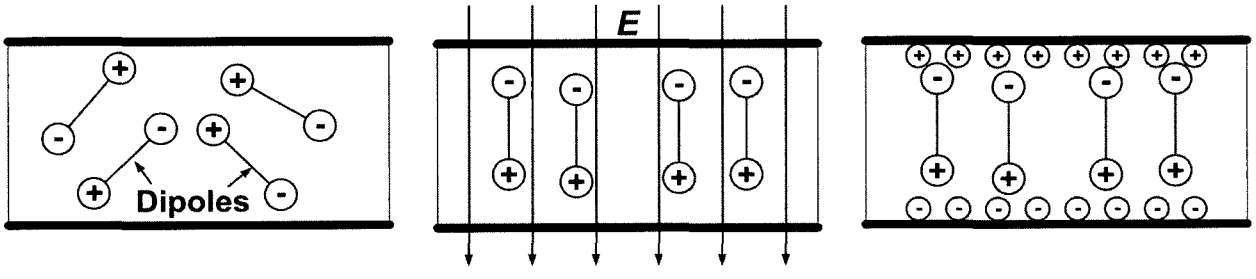

(a) A crystalline material is heated up near its Curie temperature (b) The applied electric field aligns the dipoles along the field lines (c) The polarization is permanently maintained after cooling

〈Figure 1〉 A poling process of an artificially polarized material (Fraden, 2001).

of a piezoelectric material as well as its electrical characteristics is governed by the poling direction of the material.[2] In the next section, the influence of the poling direction on Lamb waves is discussed.

2.2 The Effect of PZT Poling Directionality on Lamb Wave Propagation

In this section, it is investigated how the phase of a Lamb wave mode changes depending on (1) the poling directions of exciting and sensing PZT wafer transducers and (2) whether a wafer transducer is attached either on the top or bottom surface of a plate. For illustration, it is assumed four identical PZT wafer transducers, labeled as "A", "B", "C", and "D", are attached to the plate as shown in Figure 2 (a). The arrows indicate the positive poling directions of each PZT transducers. PZTs A and D are placed exactly at the same position but on the other side of the plate. PZTs B and C are positioned in a similar fashion. Furthermore, it is assumed that a narrow-band tone burst is applied as an input signal, and the driving frequency (150 kHz) is chosen such that only the fundamental symmetric (S_0) and anti-symmetric (A_0) modes are generated. Although only the S_0 and A_0 modes are shown here for simplicity, the proposed concept is applicable even with multiple higher modes.

When PZT A is excited, the S_0 and A_0 modes are generated and measured at PZTs B and C.[4] In an ideal condition, the amplitude and arrival time of the S_0 mode measured at PZTs B and C should be identical. In addition, both PZTs B and C should be subjected to positive bending because of the symmetric nature of the S_0 mode [See the figure on the left in Figure 2 (b)]. (In this paper, this term of "positive bending" is used when the positively polarized side of the PZT is subjected to tensile strain. On the other hand, the PZT is subjected to negative bending when the negatively polarized size of the PZT is subjected to tensile strain. The positive bending produces a "positive" output voltage while the negative bending results in a "negative" output voltage value.) Because both PZTs B and C are subject to the positive bending, the phase of the S_0 mode measured at these PZTs are identical as well as the amplitude and arrival time [See the S_0 mode in Figure 4 (a)]. As far as the A_0 mode is concerned, PZT B is subjected to the negative bending although PZT C still undergoes the positive bending [See the figure on the right in Figure 2 (b)]. Therefore, the A_0 modes measured at PZTs B and C are out-of-phase [See the A_0 mode in Figure 4 (a)]. However,

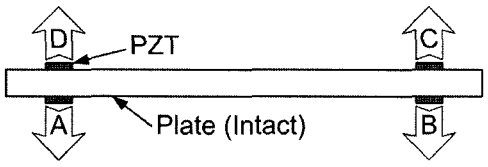

(a) Test configuration I with collocated PZTs with the opposite poling directions

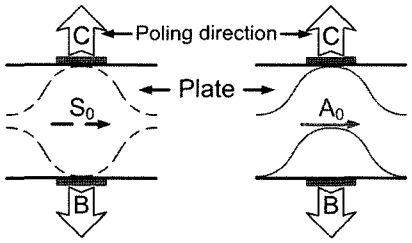

(b) The S0 mode produces the same bending for PZTs B and C while the A_0 mode results in the opposite bending

〈Figure 2〉 The effect of the PZT poling directions on the phases of the S_0 and A_0 modes (Configuration I).

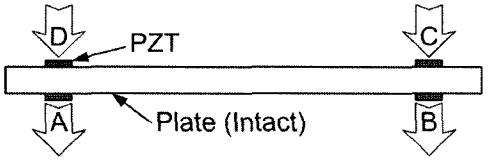

(a) Test configuration II with all PZTs with the same poling directions

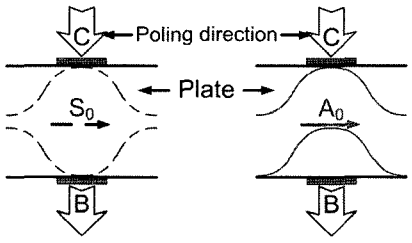

(b) The S_0 mode produces the opposite bending for PZTs B and C while the A_0 mode results in the same bending

〈Figure 3〉 The effect of the PZT poling directions on the phases of the S_0 and A_0 modes (Configuration II).

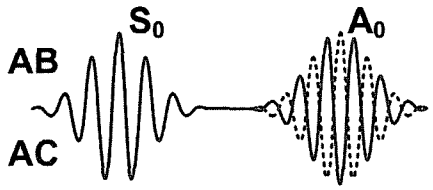

(a) S_0 and A_0 modes measured from configuration I in Figure 2 (a): S_0 modes in-phase & A_0 modes out-of-phase

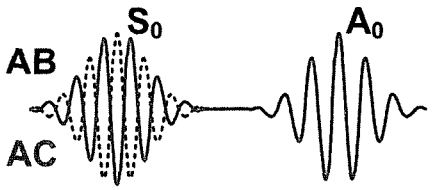

(b) S_0 and A_0 modes measured from configuration II in Figure 3 (a): S_0 modes out-of-phase & A_0 modes in-phase

〈Figure 4〉 A schematic comparison of the S_0 and A_0 modes measured from Configurations I and II shown in Figure 2 (a) and Figure 3 (a), respectively: AB (a dash line) and AC (a solid line) denote the response signals measured at PZTs B and C when a tone burst input is applied at PZT A.

when the poling direction of the PZT C is switched [Figure 3 (a)], PZTs B and C will produce out-of-phase S_0 modes and in-phase A_0 modes [Figure 3 (b) and Figure 4 (b)].

This idea of using the PZT poling directionality in Lamb wave propagation is not a completely new idea. However, the majority of the past work has focused on selective generation of S_0 and A_0 modes.[5-8] For instance, by exciting PZTs A and D shown in Figure 2 (a) in-phase, only the S_0 mode can be excited. In this study, the polarization characteristic of the PZT is utilized not only for selective generations of Lamb wave modes but also for selective measurements. In the following section, this concept is further advanced so that the mode conversion due to crack formation can be extracted from the measured Lamb wave signals.

2.3 Extracting Mode Conversed Signals Due to Crack Damage Using a PZT Poling Direction

In this subsection, the PZT polarization characteristic is further advanced so that the mode conversion due to crack formation can be detected without using any prior baseline data. First, the effect of a crack on Lamb wave modes is described. If Lamb waves propagating along a thin plate encounter a discontinuity, some portion of the waves are reflected at the discontinuity point and others are transmitted through it. When a S_0 mode arrives at the notch as shown in Figure 5, it is separated into S_0 and A_0 modes (denoted as S_0/S_0 and A_0/S_0, respectively). In a similar manner, an A_0 mode is also divided into S_0 and A_0 modes (S_0/A_0, and A_0/A_0). This phenomenon is called mode conversion.[9]

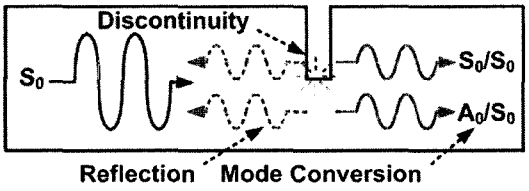

〈Figure 5〉 A schematic diagram of mode conversion and reflection due to a discontinuity on a plate.

When the plate is in a pristine condition and four identical PZTs are instrumented as shown in Figure 6 (a), it can be shown that signal AB becomes identical to signal CD as illustrated in Figure 6 (b) (Park et al.[10]). Here, signal AB denotes the response signal measured at PZT B when the excitation is applied at PZT A, and signal CD is defined in a similar fashion. However, signal AB is no longer identical to signal CD [Figure 6 (c) and (d)] when there is a crack between PZTs A and B (or PZTs C and D). As for signal AB, the S_0/A_0 mode arrives at PZT B earlier than the A_0/S_0 mode when the notch is located closer to PZT A than PZT B (assuming that the S_0 mode travels faster than the A_0 mode). Conversely, the S_0/A_0 mode arrives at PZT D after the A_0/S_0 mode in the case of signal CD. In Figure 6 (d), signals AB and CD are drawn considering not only the arrival time of each mode but also the poling directions of the PZTs.

Note that, while the S_0 and A_0 modes in Figure 6 (d) are in-phase, the S_0/A_0 and A_0/S_0 modes in signals AB and CD are fully out-of-phase. Therefore, the additional modes generated by a notch can be extracted simply by subtracting signal AB from signal CD as shown in Figure 6 (d). Because this approach relies only on comparison of two signals obtained at the current state of the system

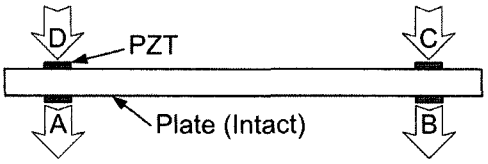

(a) An intact plate with the PZT configuration II shown in Figure 3 (a)

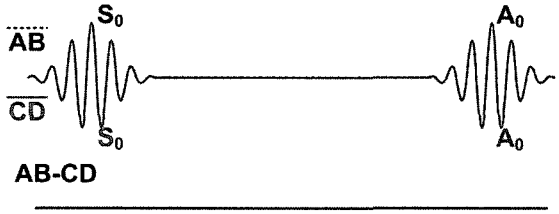

(b) Comparison of signals AB and CD without a notch: the S_0 & A_0 modes are identical

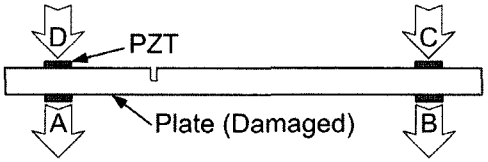

(c) A damaged plate with the PZT configuration II shown in Figure 3 (a)

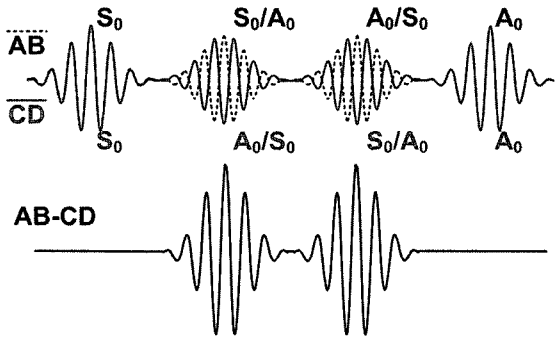

(d) Comparison of signals AB and CD with a notch: the S_0 & A_0 modes are identical, but the S_0/A_0 & A_0/S_0 modes are out-of-phase

〈Figure 6〉 Extraction of the additional Lamb wave modes generated by a notch using the poling directionality of the PZT transducers (A_0/S_0 mode denotes an A_0 converted from S_0 when it passes through a crack. S_0/A_0 is defined similarly).

rather than comparison with previously recorded reference data, it is expected that this approach reduces false alarms of defect due to changing operational and environmental variations of the system. For instance, it can be readily shown that temperature change of the system does not affect this approach.

2.4 Development of a Filter Technique to Address Variations in PZT Size, Alignment and Bonding Condition

In the previous subsection, it is shown that signals AB and CD are indistinguishable when there is no crack [Figure 6 (b)]. This is based on the assumption that all PZT transducers are identical and PZTs A and D (or PZTs B and C) are perfectly collocated. In practice, these assumptions can not be fully satisfied because of variations in PZT size, alignment and bonding condition.[10] Therefore, residual differences would remain after subtracting the two signals even at the absence of a crack, and this could be a source of positive false alarms. To tackle this practical implementation issue, a thresholding technique is developed here.

The development of this signal processing technique is based on the observation that the additional modes generated by a crack are out-of-phase while the other modes are in-phase when signals AB and CD are compared [Figure 6 (d)]. According to Figure 6 (d), because the S_0 modes and A_0 modes in signals AB and CD are in-phase, the point-by-point product (PPP) values between the S_0 modes or the A_0 modes are always positive. On the other hand, the PPP values between the S_0/A_0 mode of signal AC and the A_0/S_0 mode of signal BD (or between the A_0/S_0 mode of signal AC and the S_0/A_0 mode of signal BD) always become negative. Therefore, the existence of a crack can be detected by observing the negative PPP values between signals AB and CD. Then, it is investigated how the PPP values are affected by variations in PZT size, alignment and bonding condition. The main effects of the non-ideal PZTs on signals AB and CD can be summarized as the amplitude change of the response signals and the time shifting of one signal with respect to the other. For instance, the debonding and/or cracking of PZT A can reduce the coupling area between PZT A and the substrate and consequently decrease the amplitude

of signal AB with respect to signal CD. It can be readily shown that this pure amplitude change does not alter the sign of the PPP values. However, the variations in PZT size, alignment and bonding condition can also cause phase shifting, and this requires a special treatment.

In Figure 7, an example of the phase shift caused by PZT transducer misalignment is illustrated. The results shown in Figure 7 are obtained from the same configuration shown in Figure 3 (a) except that PZT C is shifted 0.76 mm to the right with respect to PZT B. That is, the distance between PZTs A and B becomes 0.76 mm shorter than the distance between PZTs C and D. Due to this misalignment, the A_0 mode in signal AB arrives about 0.25 μs earlier than the A_0 mode in signal CD (0.76 mm / 3.055 mm/μs = 0.25 μs) [Figure 7 (a)]. Because the A_0 mode travels slower than the S_0 mode at 150 kHz (VS = 5.088 mm/μs, V_A = 3.055 mm/μs), the A_0 mode is more severely affected by the misalignment than the S_0 mode. Therefore, the discussion here focuses on the delay of A_0 modes. Furthermore, note that 0.76 mm misalignment is equivalent to 8% of the 10 mm 10 mm PZT wafer transducer size. Although 0.25 μs may be considered a small time delay, Figure 7 (b) shows that this time delay produces a substantial difference between signals AB and CD when

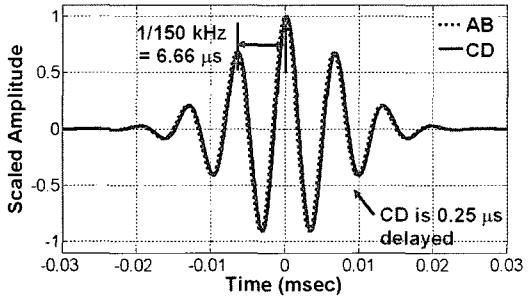

(a) Signals AB and CD when PZT C is shifted 0.76 mm to the right with respect to PZT B

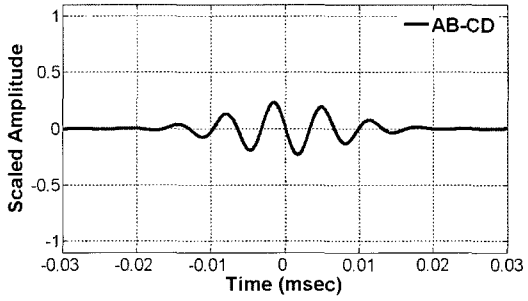

(b) Difference between signals AB and CD

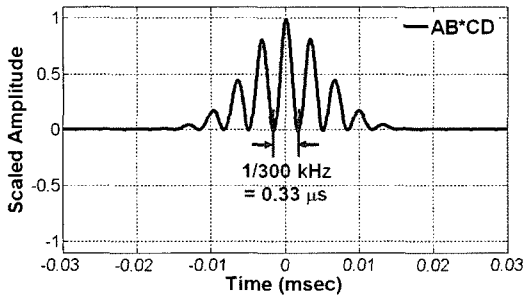

(c) The PPP values between signals AB and CD when PZT C is shifted 0.76 mm to the right wrt. PZT B

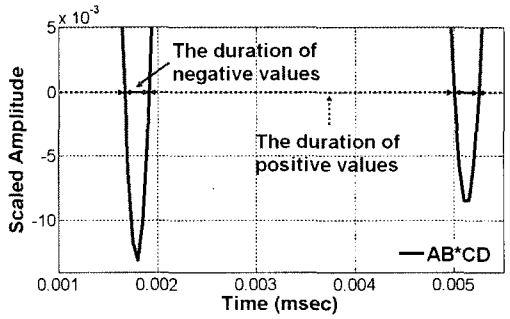

(d) Zoomed-in version of (c), indicating the durations of positive values and negative values due to misalignment

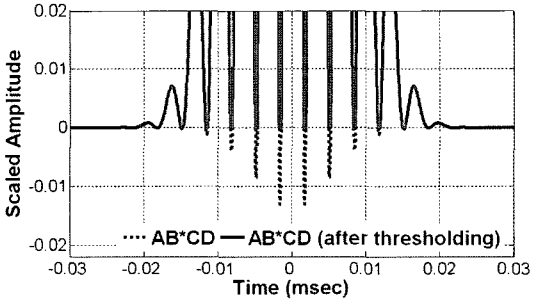

(e) Zoomed-in version of (c), highlighting the negative values of the PPP: a dash line - before thresholding, and a solid line - after thresholding

〈Figure 7〉 Compensation of sensor misalignment using the proposed thresholding process (AB*CD denote the point-by-point product (PPP) between signals AB and CD).

they are subtracted from each other.

On the other hand, Figure 7 (c) shows that the PPP values between signals AB and CD are mostly positive except at a few negative points. The negative PPP values are the results of the misalignment and amplified in Figure 7 (d). It can be analytically shown that the PPP between the two signals at 150 kHz produces a 300 kHz frequency component as shown in Figure 7 (c). Therefore, the time period of the PPP values becomes 3.33 μs (= 1/300 kHz). The observation of Figure 7 (d) further reveals that the duration of the negative PPP values is shorter than that of the positive PPP values. For instance, 3 mm misalignment, which is equivalent to 30% misalignment in a 10 mm 10 mm PZT wafer transducer, produces negative PPP values with a duration of 0.98 μs (= 3 mm / 3.055 mm/μs). Note that the mode conversion also produces negative PPP values. However, the duration of the negative PPP values caused by the mode conversion becomes 2.35 μs (= 3.33 μs - 0.98 μs) in this configuration. Therefore, the duration of the negative PPP values due to the mode conversion remains longer than the duration caused by PZT misalignment as long as the PZT misalignment is controlled under certain precision. In this paper, it is assumed that the PZT misalignment can be controlled under 30% of the 10 mm × 10 mm PZT transducer and this misalignment produces the negative PPT values with a duration less than or equal to 0.98 μs. Then, the effect of the misalignment is eliminated by removing the negative PPP values, whose duration is less than 0.98 μs [Figure 7 (e)]. The effectiveness of this thresholding technique is further investigated in the following numerical studies.

3. Numerical Simulation

The idea of using the PZT polarity for crack detection was first validated by numerical simulation. Using COMSOL Multiphysics software (www.comsol.com), Lamb wave propagation in a two dimensional aluminum plate was simulated using the combination of plain strain, piezo plain strain, and electrostatics modules in COMSOL software. The length of the plate was 70 cm, and its thickness was 6 mm. Four identical PZTs with a size of 10 mm × 10 mm × 0.508 mm were attached to the plate model as shown in Figure 8. Note that PZTs A and D were collocated but on the other side of the plate with the same poling direction. PZTs B and C were placed in a similar fashion. The parameter values used in the numerical simulation are listed in Table 1. A narrowband tone-burst signal at 150 kHz was used as an input signal. In the simulation, Rayleigh damping coefficients were set to 10^{-4} for a mass damping coefficient and 0 for a stiffness damping coefficient, respectively. The simulation results were obtained from a time dependent solver, and a time step was set to 0.25 μs, which is equivalent to 4 M samples/sec. To control the error in each integration step, relative tolerance and absolute tolerance for the solution were chosen to be 10^{-3} and 10^{-10}, respectively. The maximum backward differentiation formula (BDF) order for setting the degree of the interpolating polynomials in the time-stepping method was set to order 2. Finally, the model was meshed using a mapped mesh option, and the size of each mesh was limited to 1 mm 1 mm.[11]

Figure 9 illustrates that signals AB and CD were almost identical and this well corresponds to the theoretical expectation. Once a notch of 3 mm depth and 1 mm width was introduced 100 mm away from PZT D toward

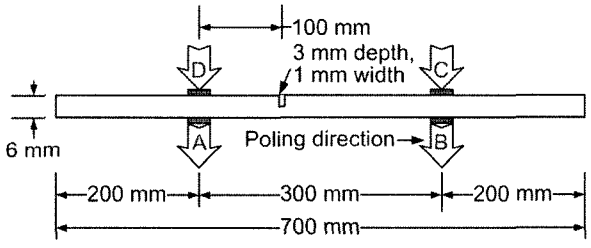

〈Figure 8〉 Dimension of an aluminum plate used in numerical simulation

〈Table 1〉 Parameters used in numerical simulation.

Exciting frequency	150 kHz
α (Mass damping coefficient)	10^{-4}
β (Stiffness damping coefficient)	0
Sampling rate	4 Ms/s
Relative tolerance	10^{-3}
Absolute tolerance	10^{-10}
Maximum BDF order	2
Mesh size (mapped mesh)	1 mm×1 mm maximum

PZT C, signal AB became different from signal CD as a result of the mode conversion induced by the crack [Figure 10 (a)]. Then, the mode conversion due to crack formation was extracted simply by subtracting signal CD from signal AB [Figure 10 (b)].

So far it has been assumed that all PZTs are identical, and two PZTs on the both sides of the beam are precisely collocated. In practice, the size, bonding condition and electrical impedance of PZT transducers will vary from one device to another, and there can be PZT misalignment. To investigate the effectiveness of the proposed thresholding techniques for addressing these practical implementation issues, the previous numerical simulation was repeated after introducing misalignment between PZTs B and C: PZT C was shifted 1 mm to the right with respect to PZT B. Although the shapes of signals AB and CD were almost identical as shown in Figure 11 (a), their subtraction produced residuals [Figure 11 (b)], whose amplitudes were much higher compared to the one in Figure 9 (b). Figure 12 (a) shows the PPP values

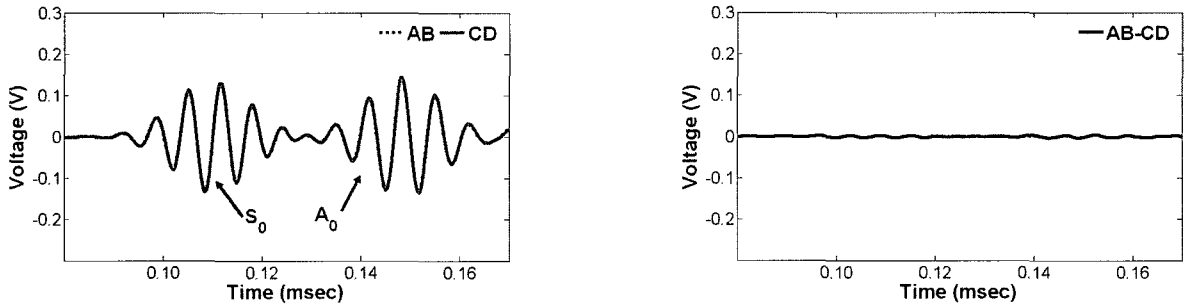

(a) Signals AB and CD without a notch

(b) Difference between signals AB and CD

〈Figure 9〉 Simulated Lamb wave signals without notch.

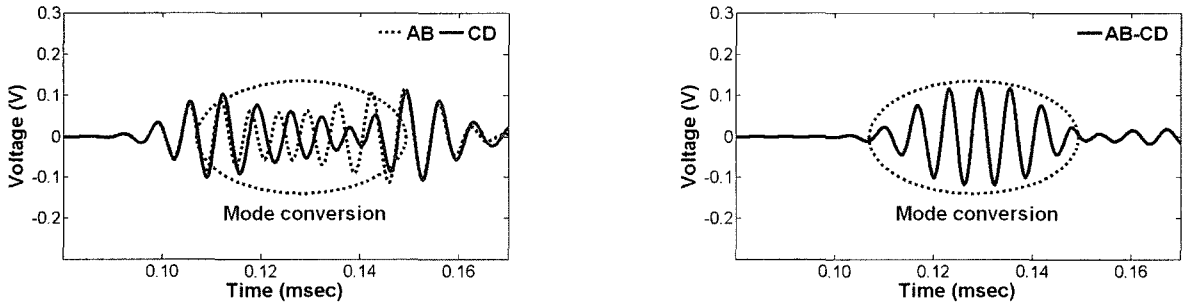

(a) Signals AB and CD with a notch (3 mm depth, 1 mm width)

(b) Difference between signals AB and CD with a notch (3 mm depth, 1 mm width)

〈Figure 10〉 Simulated Lamb wave signals with a notch of 3 mm depth and 1 mm width.

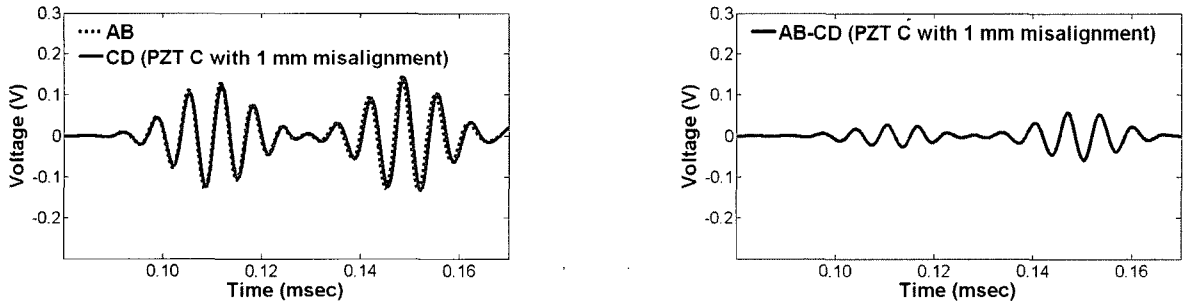

(a) Signals AB and CD with PZT C shifted 1 mm to the right wrt PZT B

(b) The difference between signals AB and CD with PZT C shifted 1 mm to the right wrt PZT B

〈Figure 11〉 The effect of PZT misalignment on the difference between signals AB and CD (PZT C shifted 1 mm to the right with respect to PZT B).

between signals AB and CD, and the negative PPP values were magnified in Figure 12 (b). By determining the duration of the negative PPP values and removing negative values whose duration is less than the threshold value (0.98 μs defined in Section 2.4.), the effect of the PZT misalignment was removed in Figure 12 (b).

In Figure 13 (a), the numerical simulation was repeated again with a crack introduced at 100 mm away from PZT A toward PZT B as well as the PZT misalignment. Subtracting signal AB from signal CD produced the residual signal shown in Figure 13 (b). Without relying on prior baseline data, it is challenging to determine whether this remaining signal appears due to mode conversion or sensor misalignment. However, by calculating the PPP between signals AB and CD and applying the proposed thresholding technique, the mode conversion

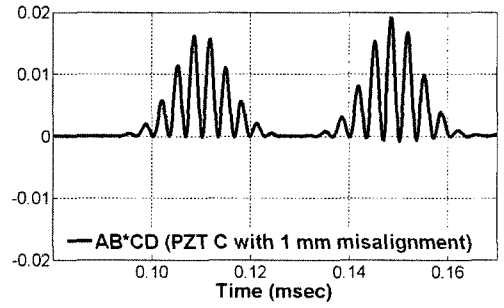

(a) The PPP values between signals AB and CD when PZT C is shifted 1 mm to the right wrt to PZT B

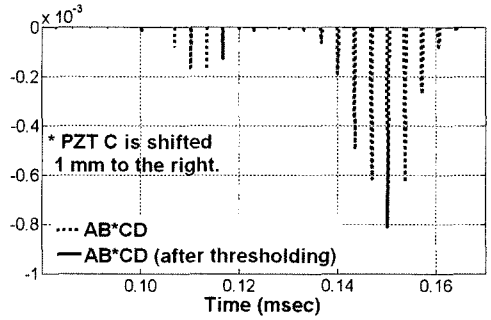

(b) Negative PPP values between signals AB and CD before and after applying the proposed thresholding

〈Figure 12〉 Compensation of the PZT transducer misalignment using the proposed thresholding technique (PZT C: shifted 1 mm to the right with respect to PZT B, without a notch).

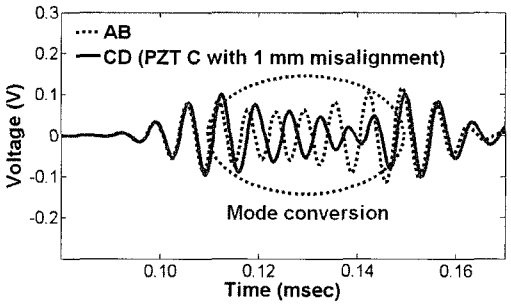

(a) Signals AB and CD with PZT C shifted 1 mm to the right and a 3 mm depth notch

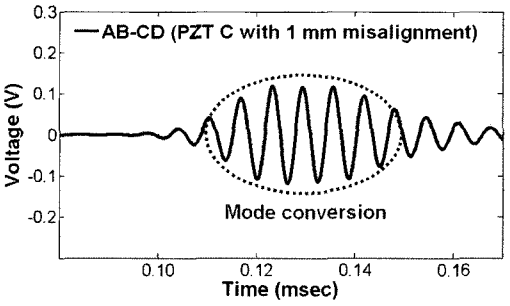

(b) Difference between signals AB and CD with PZT C shifted 1 mm to the right and a 3 mm depth notch

〈Figure 13〉 Comparison of signals AB and CD with PZT transducer misalignment and a 3 mm depth notch.

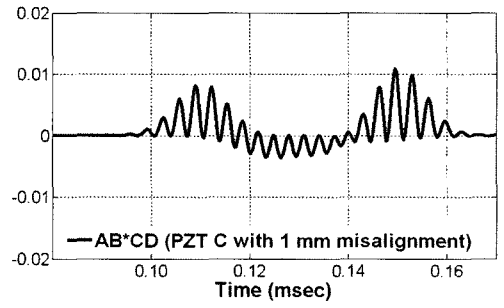

(a) The PPP values between signals AB and CD with PZT C shifted 1 mm to the right and a 3 mm depth notch

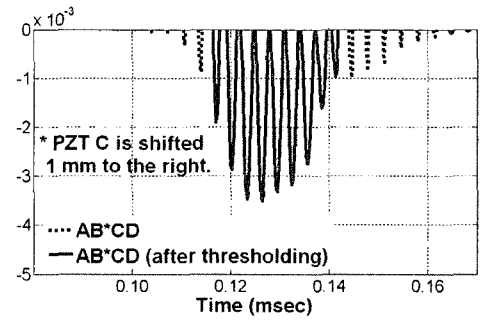

(b) Negative PPP values between signals AB and CD before and after applying the proposed thresholding

〈Figure 14〉 The extraction of the mode conversion using the proposed thresholding technique at the presence of the PZT transducer misalignment (PZT C: shifted 1 mm to the right with respect to PZT B and a 3 mm depth notch).

due to a crack was extracted as shown in [Figure 14 (a) and (b)]. This numerical example demonstrates that crack formation can be identified even when there is PZT transducer misalignment. This numerical finding is further substantiated in the following experimental study.

4. Experimental Results

4.1 Description of Experimental Setup

To further examine the proposed reference-free NDT technique, experimental tests have been conducted on an aluminum plate. The overall test configuration of the experiment and the test specimen are shown in Figure 15. The data acquisition system was composed of an arbitrary waveform generator (AWG), a high-speed signal digitizer (DIG), a low noise preamplifier (LNP) and a multiplexer. The dimension of the plate was 122 cm × 122 cm × 0.6 cm, and four PSI-5A4E type PZT wafer transducers (1.0 cm × 1.0 cm × 0.0508 cm) were mounted in the middle of the plate. PZTs A and D were collocated and attached on the different side of the plate, and PZTs B and C were mounted in a similar fashion. The PZTs were attached so that their poling directions were identical to the configuration shown in Figure 3 (a). PZTs A and B (or PZTs C and D) were 0.52 m apart each other. In this experiment, the PZT transducers were attached to either the top or the bottom surface of the plate with a commercial cyanoacrylate adhesive.

Using the 14-bit AWG, a tone-burst signal with a ± 10 peak-to-peak voltage and a driving frequency of 150 kHz was generated and applied. First, PZT A in Figure 15 (b) was excited using the tone-burst waveform. Then, PZT A generated elastic waves, and the response was measured at PZT B. When the waves arrived at PZT B, the voltage output from PZT B was amplified by the LNP with a gain of fifty and measured by the DIG. The sampling rate and resolution of the DIG were 20 MS/sec and 16 bits, respectively. In order to increase a signal-to-noise ratio, the forwarding signals were measured twenty times and averaged. After the forwarding signal from PZT A to PZT B (signal AB) was measured, the same process was repeated by exciting PZT C and measuring response at PZT D (signal CD). Finally, the PPP values between signals AB and CD were calculated, and the negative PPP values due to sensor misalignment were selectively removed using the proposed thresholding technique. Detailed test results are described in Section 4.2.

4.2 Crack Detection

In Figure 16 (a), Lamb wave signals obtained from an intact plate are presented. Using the test setup described in 4.1, signals AB and CD were measured. Although signal AB was supposed to be identical to signal CD, a residual signal was observed in Figure 16 (b) due to variations in PZT alignment, size and bonding condition.

Then, a 1 mm (width) × 60 mm (length) notch was introduced between PZTs A and B (150 mm away from PZT A toward PZT B), and its depth was gradually

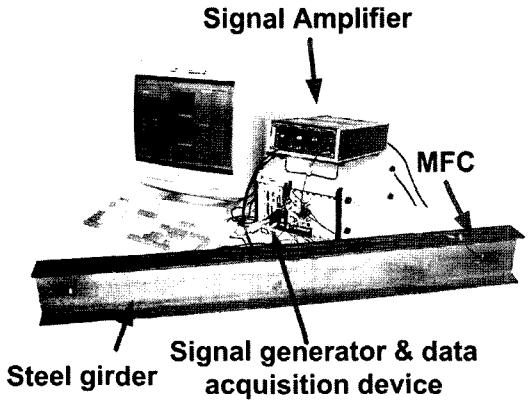

(a) A data acquisition system

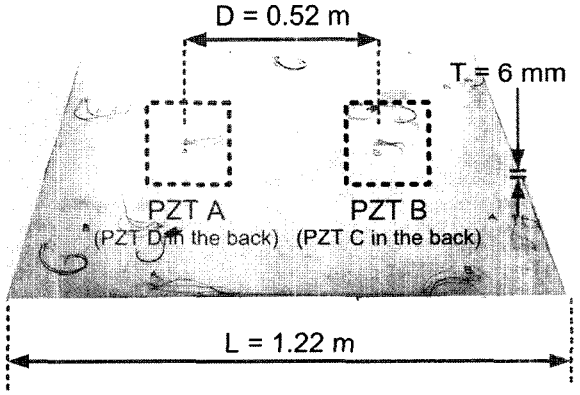

(b) A square aluminum plate

〈Figure 15〉 Testing configuration for detecting a crack on an aluminum plate.

increased up to 3 mm. Due to crack formation, two additional modes appeared between the existing S_0 and A_0 modes as shown in Figure 16 (d), (f) and (h). The comparison of Figure 16 (b) with Figure 16 (f) and (h) clearly shows the effect of the mode conversion on the difference between signals AB and CD. However, the existence of the mode conversion may not be conclusive for the 1 mm depth notch shown in Figure 16 (d) unless it is compared with the signal in Figure 16 (b).

Next, the PPT values between signals AB and CD were computed and the proposed thresholding technique was applied. Using the proposed thresholding technique, the negative values associated with the PZT variations were selectively removed while the negative PPP values

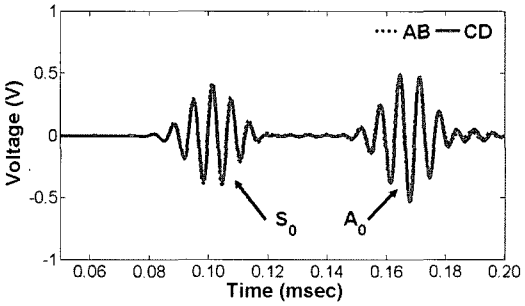

(a) Signals AB and CD without a notch

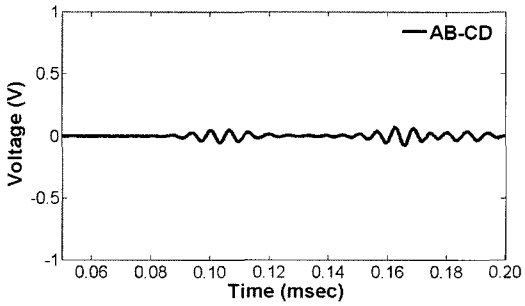

(b) Difference between signals AB and CD without a notch

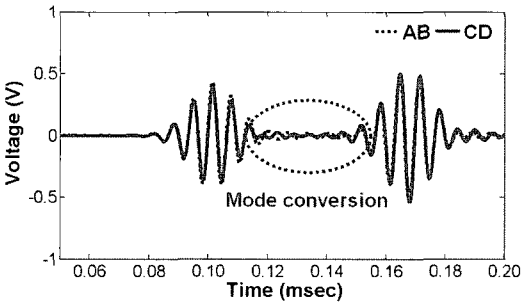

(c) Signals AB and CD with a 1 mm notch

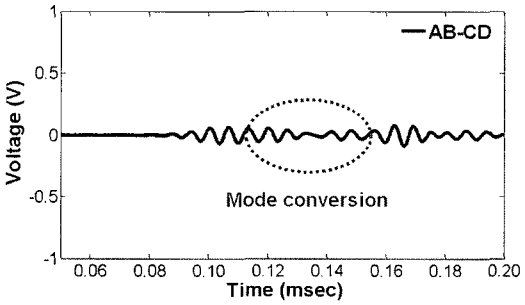

(d) Difference between signals AB and CD with a 1 mm notch

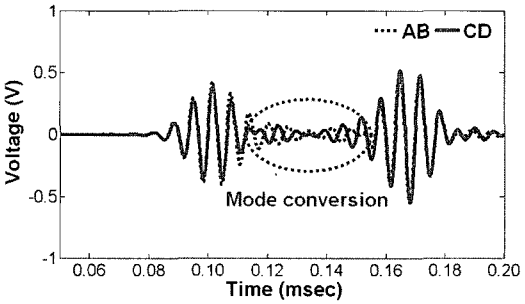

(e) Signals AB and CD with a 2 mm notch

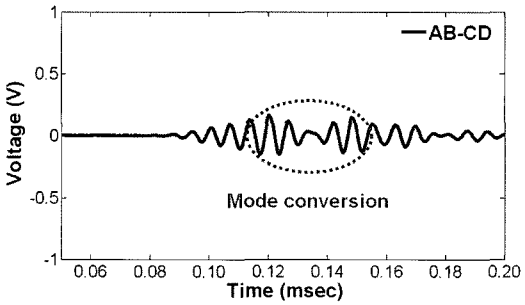

(f) Difference between signals AB and CD with a 2 mm notch

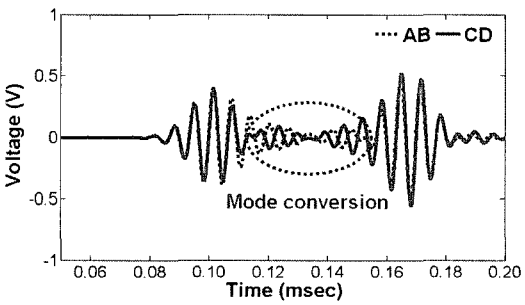

(g) Signals AB and CD with a 3 mm notch

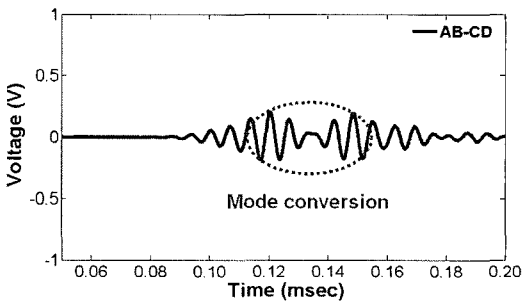

(h) Difference between signals AB and CD with a 3 mm notch

〈Figure 16〉 Comparison of signals AB and CD by increasing the depth of a notch.

resulted from the mode conversion were preserved. As shown in Figure 17 (a), the negative PPP values corresponding to the intact condition became negligible after applying the thresholding technique. Once the notch was introduced, the effect of the two additional modes clearly appeared as shown in Figure 17 (b), (c), and (d). Note that even the existence of the incipient notch (1 mm) was clearly detected [Figure 17 (b)], and the arrival times of these two additional modes in Figure 17 (b), (c), and (d) well matched with the theoretical calculation.

In addition, an attempt was made to estimate the location of the notch by measuring the arrival times of the two converted modes in signals AB and CD. Based on signal AB in Figure 16 (a), the group velocities of the S0 and A0 modes were estimated to be 5.128 m/ms and 3.099 m/ms (theoretically, V_S = 5.088 m/ms and V_A = 3.055 m/ms), respectively. Assuming that the notch is closer to the PZT A, the arrival time of the first converted mode, t_a, was estimated using Eq. (1):

$$t_a = \frac{s}{V_A} + \frac{l-s}{V_S} \tag{1}$$

where s and l denote the distances between the notch and PZT A and between PZT A and PZT B, respectively. V_A, V_S, denote the group velocities of the A_0 and S_0 modes. By measuring the arrival time of the first converted mode (0.1206 ms) and using Eq. (1), the two possible locations of the notch were estimated to be at 15.034 cm away from PZT A or PZT B. This estimated distance was close to the actual notch location (0.2% error).

Note that, when a notch is closer to PZT A than PZT B, the S_0/A_0 mode arrives at PZT B earlier than the A_0/S_0 mode. Conversely, the A_0/S_0 arrives first when the notch is closer to PZT B. However, it could not be determined whether the first arrived mode on each signal was the S_0/A_0 mode or the A_0/S_0 mode, because these modes were not distinguishable [Figure 6 (d)]. (When signals AB and CD are compared, both modes are out-of-phase) Therefore, it was only possible to narrow down the crack position into two alternatives. In this

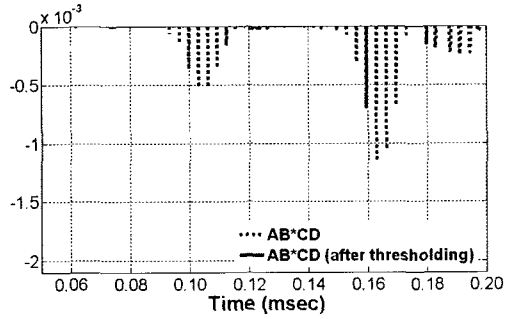

(a) Negative PPP values between signals AB and CD before and after applying the proposed thresholding (without a notch)

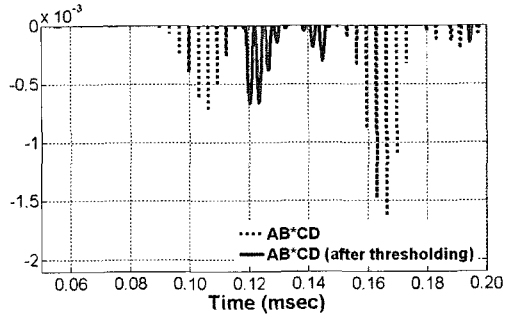

(b) Negative PPP values between signals AB and CD before and after applying the proposed thresholding(with a 1 mm depth notch)

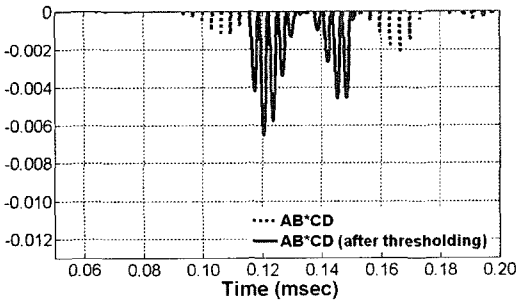

(c) Negative PPP values between signals AB and CD before and after applying the proposed thresholding (with a 2 mm depth notch)

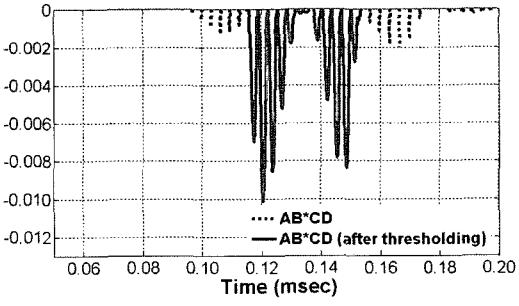

(d) Negative PPP values between signals AB and CD before and after applying the proposed thresholding (with a 3 mm depth notch)

〈Figure 17〉 The extraction of the mode conversion produced by a notch using the proposed thresholding technique at the *presence of the PZT transducer misalignment.*

example, the crack location was determined assuming that the crack was closer to PZT A. However, the S_0/A_0 and A_0/S_0 modes could have been distinquished if signals AB and AC had been compared instead of signals AB and CD. When signals AB and AC are compared, the S_0/A_0 and A_0/S_0 modes become out-of-phase and in-phase, respectively. Therefore, each mode can be selectively identified. Once each mode is identified, the crack location along the wave propagation path can be uniquely determined.

5. Conclusion

A new concept of nondestructive testing is developed in this study so that crack formation in a thin metal structure can be instantaneously detected without referencing to previously stored baseline data. This reference-free technique for crack detection is developed based on Lamb wave propagations and PZT polarization characteristics. When Lamb waves propagate through a crack, the Lamb wave modes are converted to other modes, and this phenomenon is called mode conversion. The appearance of this mode conversion is identified by strategically placed PZT wafer transducers considering the poling directions of individual PZTs. Numerical simulations and experimental tests conducted in this study substantiate the effectiveness of the proposed reference-free technique for crack detection. Practical instrumentation issues such as variations in PZT size, bonding condition as well as alignment are addressed by developing a thresholding technique. Because this reference-free technique does not rely on previously obtained baseline data for crack detection, it is expected that this approach minimize false alarms of damage due to changing operational and environmental variations experienced by in-service structures. This robustness of the proposed technique against undesirable variations in the system, such as temperature and external loading, can make it attractive for long-term continuous monitoring. Further investigation is underway to extend the proposed concept to more complex structures such as steel girders and welded connections and to perform field testing at a bridge site.

Acknowledgement

This work was supported by the National Science Foundation under grants CMS-0529208 and the Pennsylvania Infrastructure Technology Alliance (PITA), a partnership of Carnegie Mellon University, Lehigh University and the Commonwealth of Pennsylvania Department of Community and Economic Development. The authors like to acknowledge Dr. S. Liu for the NSF support and Prof. Gary K. Fedder for PITA support.

References

1. Fraden, J., *Handbook of Modern Sensors*, 2nd Edition, American Institute of Physics, 2001, 556pp.
2. Buchanan, R.C., *Ceramic Materials for Electronics*, 3rd Edition, Marcel Dekker, New York, 2004, 676pp.
3. Giurgiutiu, V. and Zagrai, A.N., "Characterization of Piezoelectric Wafer Active Sensors," *Journal of Intelligent Material Systems and Structures*, Vol. 11, No. 12, 2000, pp. 959-976.
4. Viktorov, I., *Rayleigh and Lamb Waves*, Plenum Press, New York, 1967, 154pp.
5. Su, Z. and Ye, L., "Selective generation of Lamb wave modes and their propagation characteristics in defective composite laminates," *Proceedings of the Institution of Mechanical Engineers, Part L: Journal of Materials: Design and Applications*, Vol. 218, No. 2, 2004, pp. 95-110.
6. Yamanaka, K., Nagata, Y. and Koda, T., "Selective excitation of single-mode acoustic waves by phase velocity scanning of a laser beam," *Applied Physics Letters*, Vol. 58, No. 15, 1991, pp. 1591-1593.
7. Wilcox, P.D., Lowe, M.J.S. and Cawley, P., "Mode and Transducer Selection for Long Range Lamb Wave Inspection," *Journal of Intelligent Material Systems and Structures*, Vol. 12, No. 8, 2001, pp. 553-565.
8. Giurgiutiu, V., "Tuned Lamb Wave Excitation and Detection with Piezoelectric Wafer Active Sensors for Structural Health Monitoring," *Journal of Intelligent Material Systems and Structures*, Vol. 16, No. 4, 2005, pp. 291-305.
9. Cho, Y., "Estimation of Ultrasonic Guided Wave Mode Conversion in a Plate with Thickness Variation," *IEEE transactions on Ultrasonics*, Ferroelectrics, and Frequency Control, Vol. 47, No. 3, 2000, pp. 591-603.
10. Park, H.W., Kim, S.B, and Sohn, H., "Understanding a Time Reversal Process in Lamb Wave Propagations," *Proceedings on Structural Control and Health Monitoring*, 2006.
11. COMSOL AB., "COMSOL Multiphysics User's Guide," Version 3.2, 2005.